Surface Science 605 (2011) 1994–1998

Contents lists available at ScienceDirect

Surface Science

journal homepage: www.elsevier.com/locate/susc

Terephthalic acid adsorption on Si(111)-($\sqrt{3}\times\sqrt{3}$)-Bi surfaces: Effect of Bi coverage

T. Suzuki [a,b], T. Lutz [a], G. Costantini [a,c,*], K. Kern [a,d]

[a] Max-Planck-Institut für Festkörperforschung, Heisenbergstraße 1, D-70569 Stuttgart, Germany
[b] Department of Electronics Engineering and Computer Science, Fukuoka University, Nanakuma 8-19-1, Jyonan, Fukuoka 814-0180, Japan
[c] Department of Chemistry, University of Warwick, Coventry, CV4 7AL, UK
[d] Institut de Physique de la Matière Condensée, Ecole Polytechnique Fédérale de Lausanne, CH-1015 Lausanne, Switzerland

ARTICLE INFO

Article history:
Received 12 April 2011
Accepted 25 July 2011
Available online 31 July 2011

Keywords:
Scanning tunneling microscopy
Supramolecular self-assembly
Si-metal surface alloys

ABSTRACT

The influence of the density of metallic atoms on the formation of supramolecular structures onto Si surface alloys is investigated by scanning tunneling microscopy. Terephthalic acid (TPA) adsorption experiments are performed on the Si(111) α- and β-($\sqrt{3}\times\sqrt{3}$)-Bi surfaces. Although both surfaces have the same unit cell with Bi atoms incorporated into the Si substrate, they show a completely different behavior in respect to the formation of the supramolecular arrays. TPA molecules do not build any regular structure and adsorb randomly on the α surface but self-assemble into ordered and extended layers on the β surface. This demonstrates that the absence of dangling bonds in metal-Si surface alloys is not a sufficient condition for supramolecular self-assembly but that the surface density of metallic atoms is a further essential parameter.

1. Introduction

Organic–inorganic semiconductor hybrid systems have recently attracted much attention as possible platforms for the development of devices with applications in optoelectronics, sensors and diagnostics. They could in fact benefit from the combination of various properties of both organic and inorganic materials like cheap, simple processing and high stability. Such hybrid systems generally utilize thin films of functionalized organic molecules grown on inorganic Si semiconductor substrates. An essential requirement for the fabrication of high quality molecular layers is the passivation of the Si dangling bonds, which is typically done by terminating the substrate with hydrogen or metallic atoms. This operation is necessary because of the extremely high reactivity of Si dangling bonds which can either suppress the diffusivity of the organics species or even break their molecular structure through the formation of Si–C covalent bonds.

Terephthalic acid ($C_6H_4(COOH)_2$, TPA), shown in the inset of Fig. 1(c), is a functional molecule often used in crystal engineering, in particular as elementary building block in the fabrication of metal-organic frame-works (MOF) for its ability to coordinate metal centers. Due to its multifunctional carboxylic moieties and its planar geometry, TPA, or its deprotonated terephthalate form, has also been employed as synthon for the formation of two-dimensional (2D) supramolecular structures supported on solid substrates [1–4]. In particular, rectangular-symmetry 2D MOFs have been produced on metallic surfaces by coordination with various *d*-transition metal atoms [4–12].

TPA adsorption on semiconductor surfaces such as the clean Si(111)-7×7 and the Si(111)-$\sqrt{3}\times\sqrt{3}$-Ag (hereafter denoted as 7×7 and $\sqrt{3}$-Ag, respectively) has been previously investigated [4]. TPA molecules adsorb randomly on the 7×7 surface due to a strong binding with Si dangling bonds. On the contrary, they form a supramolecular layer stabilized by intermolecular hydrogen bonds on the $\sqrt{3}$-Ag surface where the Si dangling bonds are passivated by the binding with Ag atoms. However, the successive Fe deposition does not induce the formation of any 2D MOF nor of any other type of metal–organic complex, as would be expected on metal substrates [5–9,11–13]. This has been assigned to the preference of Fe to form iron–silicide clusters instead of inducing the deprotonation and coordinating with the carboxylate moieties of TPA.

In the present study, the Si(111) α- and β-($\sqrt{3}\times\sqrt{3}$)-Bi surfaces were used as substrates (denoted as α$\sqrt{3}$-Bi and β$\sqrt{3}$-Bi, hereafter). The main difference between them is the Bi coverage [14–19]. On the α$\sqrt{3}$-Bi surface (high temperature monomer phase), Bi adatoms are located on so-called T_4 sites and their coverage is 1/3 of a monolayer (ML), as shown in Fig. 1(a). In contrast, on the β$\sqrt{3}$-Bi surface (low temperature trimer phase), Bi trimers are located on the T_4 sites and the Bi coverage is 1ML, as shown in Fig. 2(a). Only Bi atoms exist on the topmost surface layer, and there are no Si dangling bonds on both the α$\sqrt{3}$-Bi and the β$\sqrt{3}$-Bi surfaces.

To the best of our knowledge only few studies have investigated the adsorption of organic molecules on the Bi/Si(111) substrate, all of them concentrating on the aromatic hydrocarbon pentacene [20,21]. Moreover, the results are contradictory since, on the one hand, it is stated that pentacene adsorbs disorderly on α$\sqrt{3}$-Bi but forms an

* Corresponding author at: Department of Chemistry, University of Warwick, Coventry, CV4 7AL, UK.
E-mail address: g.costantini@warwick.ac.uk (G. Costantini).

0039-6028/$ – see front matter © 2011 Elsevier B.V. All rights reserved.
doi:10.1016/j.susc.2011.07.017

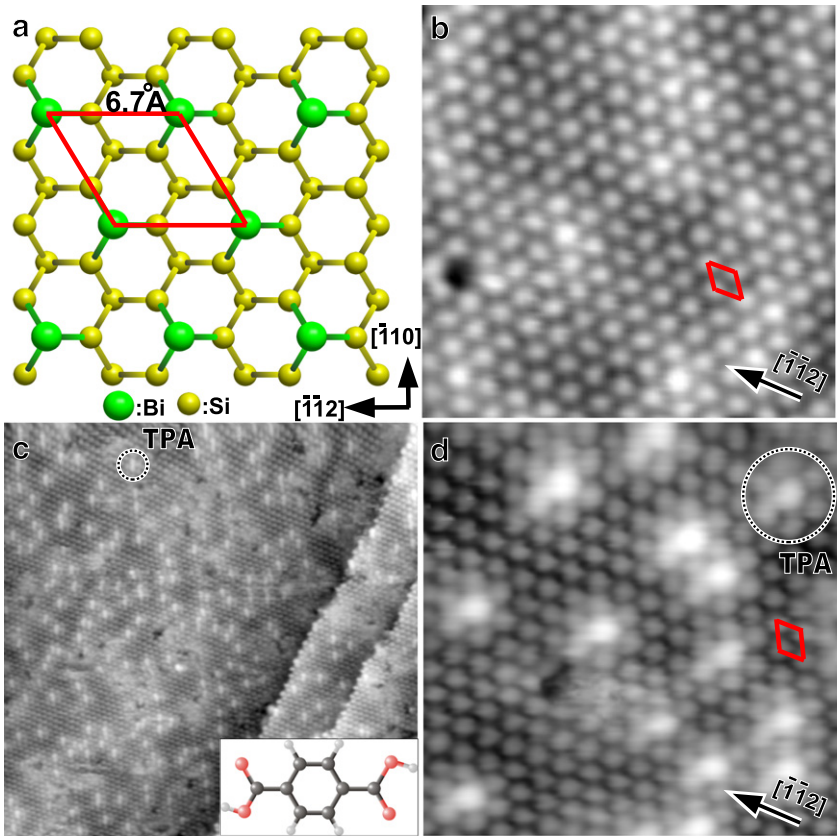

Fig. 1. (a) Schematic drawing of the $\alpha\sqrt{3}$-Bi reconstruction, (b) filled-state STM image before TPA deposition, (c) overview and (d) enlarged STM images after the TPA deposition on the $\alpha\sqrt{3}$-Bi substrate. The inset in (c) shows a schematic drawing of the TPA structure. Sizes of the STM images are (b) 10×10 nm^2, (c) 50×50 nm^2 and (d) 10×10 nm^2. Sample bias (V_s) = (b) −1.6 V, (c) and (d) −1.2 V. Tunneling current (I) = 0.2 nA. A weak tip-artifact is responsible for the elongated appearance of the TPA molecules in (c) and (d).

ordered layer of up-standing molecules on $\beta\sqrt{3}$-Bi [20] while, on the other, it is reported that regular up-standing pentacene films develop on the $\alpha\sqrt{3}$-Bi surface [21].

2. Experimental

The experiments were performed with a home-built scanning tunneling microscope (STM) operating at room temperature. The experimental procedure for the preparation of the Si substrates is described in reference [4]. Bismuth was deposited onto the clean Si surface from a molybdenum crucible heated by electron bombardment. The $\alpha\sqrt{3}$-Bi and the $\beta\sqrt{3}$-Bi reconstructions were obtained by depositing ~1ML of Bi onto the Si substrate held at about 600–650 °C and 450–500 °C, respectively [21–23]. At the higher temperatures, because of Bi desorption, only 1/3ML Bi remains on the surface. The TPA molecules (≥99%, powder, Fluka) were deposited onto the substrate at room temperature from a heated glass crucible. STM measurements were performed at room temperature in constant current mode with negative sample bias (V_s) between −0.2 V and −1.5 V (occupied states imaging).

3. Results and discussions

A schematic drawing of the surface reconstruction and a filled-state STM image of the $\alpha\sqrt{3}$-Bi surface are shown in Fig. 1(a) and (b), respectively. The Bi adatoms indicated as green spheres in 1(a), are reported to be located on the T_4 sites of the Si substrate [14–19]. Hence, they can bind with the Si surface atoms and passivate all Si dangling bonds on the substrate. The unit cell is marked by red lines in both 1(a) and 1(b). As previously reported, the Bi adatoms appear bright in the filled-state STM image in 1(b), consistently with theoretical STM image simulations based on density functional theory calculations [18,19]. A few defects are observable on the substrates, which might be related to missing Bi adatoms or to the electronic influence from dopants in the Si wafer.

Fig. 1(c) shows an STM image after the adsorption of TPA on the $\alpha\sqrt{3}$-Bi substrate. Many bright spots, one is marked by a dotted circle, are seen on the surface. They correspond to randomly adsorbed TPA molecules, without the evidence of any ordered supramolecular arrangement. This distribution is typical of a strong molecule–substrate interaction and an extremely reduced surface diffusivity where molecules adsorb very close to their impinging site. An analogous type of adsorption was observed for TPA on the bare Si(111)-7×7 substrate [4], although no dangling bonds exist on the $\alpha\sqrt{3}$-Bi surface. These results are also reminiscent of those in reference [20], where pentacene molecules are reported to adsorb disorderly on the $\alpha\sqrt{3}$-Bi substrate.

Fig. 1(d) shows an enlarged STM image of the TPA molecules on the $\alpha\sqrt{3}$-Bi substrate. The unit cell is marked by red lines in the right hand side of the figure. The TPA molecules, one is denoted by a dotted circle, have a flower-like appearance with one central bright feature and six surrounding faint features located at the position of the underlying Bi atoms. The size of TPA (~7 Å) is smaller than that of the "flower" (~14 Å), indicating a spatially extended modification of the substrate electronic properties upon molecular adsorption. Our measurements do not allow a definitive conclusion about the precise configuration of TPA. Since the absence of dangling bonds makes the formation of covalent Si–C bonds highly unlikely, the molecules are most probably intact. TPA could adopt a standing geometry, as postulated for pentacene on the α and $\beta\sqrt{3}$-Bi substrates [20,21], although a planar adsorption can not be excluded. On the contrary,

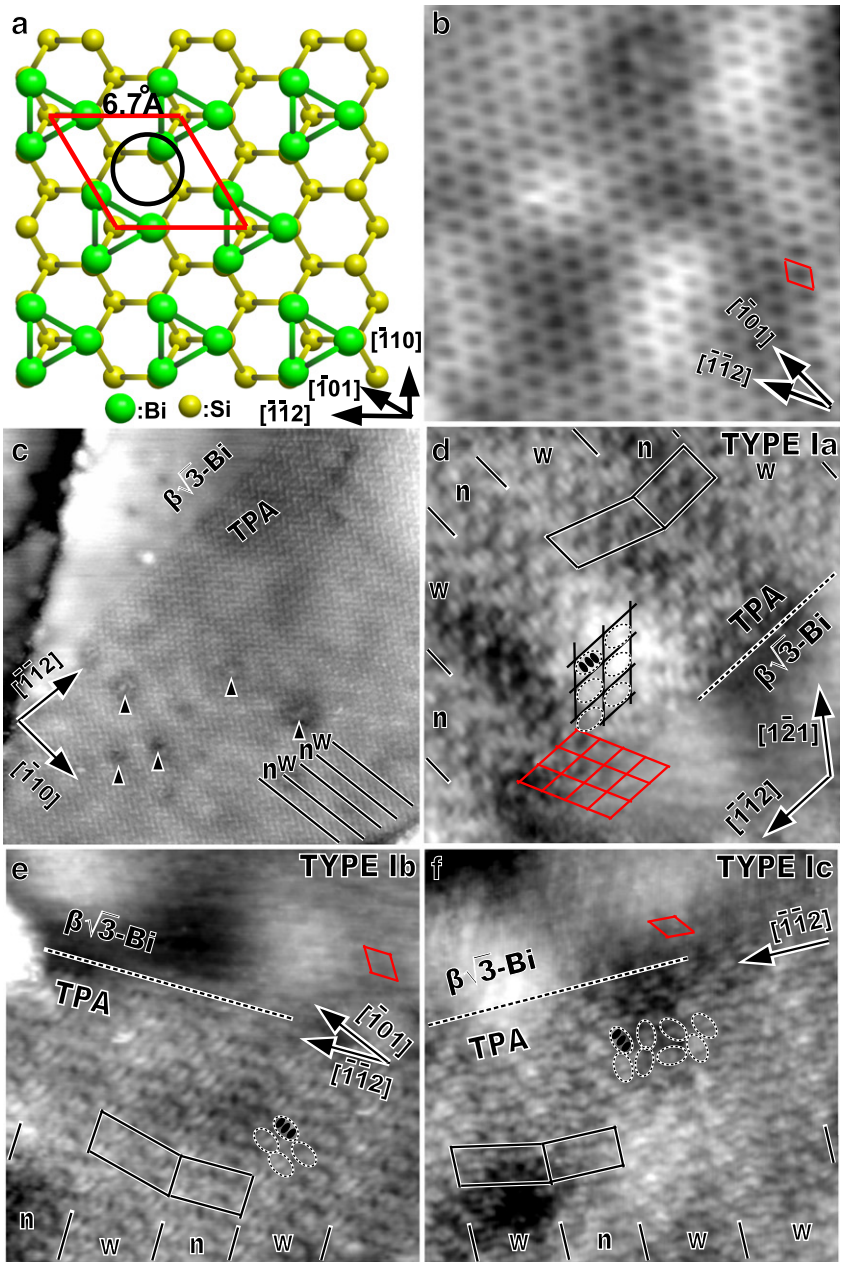

Fig. 2. (a) Schematic drawing of the $\beta\sqrt{3}$-Bi reconstruction. (b) and (c)-(f) filled-state STM images of the $\beta\sqrt{3}$-Bi substrate before and after the deposition of TPA, respectively. (d)–(f) show TYPE Ia, Ib and Ic TPA supramolecular layers, respectively. The unit cells of the narrow "n" and wide "w" regions are indicated by a rectangle and a parallelogram in (d), respectively, and straight lines identify their boundaries. The lattice of the $\beta\sqrt{3}$-Bi reconstruction is indicated by red lines. Sizes of the STM images are (b) 10×10 nm^2, (c) 50×50 nm^2 and (d)–(f) 10×10 nm^2 [V_s = (b) −0.95 V, (c) −1.6 V and (d) –(f) −0.2 V, I = 0.2 nA].

the faint features surrounding the central adsorption site observed in STM are similar to what reported for the deposition of 2,4,6-tri(2′-thienyl) 1,3,5-triazine on Si(111)-$\sqrt{3}\times\sqrt{3}$R30°-B, where a flat-lying configuration was confirmed by density functional theory calculations [24].

A schematic drawing of the surface reconstruction and a filled-state STM image of the $\beta\sqrt{3}$-Bi surface are shown in Fig. 2(a) and (b), respectively. The higher density of Bi atoms that characterizes this surface is accounted for by Bi trimers instead of the Bi adatoms located on the T_4 sites, as shown in Fig. 2(a) [14–19]. The unit cell is marked by red lines in Fig. 2(a) and Fig. 2(b). The filled-state STM image in Fig. 2(b) shows a honeycomb pattern, as reported previously [15]. Theoretical calculations suggest that the dark points of the honeycomb pattern (center of the unit cell) correspond to the center of four Bi-trimers indicated by the black circle in Fig. 2(a) [18,19]. Similar to the $\alpha\sqrt{3}$-Bi surface a few defects can be observed on the substrate.

Fig. 2(c) shows a typical STM image after TPA deposition on $\beta\sqrt{3}$-Bi. It is clear that the TPA molecules form a well-ordered supramolecular layer unlike on the $\alpha\sqrt{3}$-Bi substrate. This indicates a much weaker molecule–substrate interaction and a higher molecular diffusivity on the $\beta\sqrt{3}$-Bi surface than on $\alpha\sqrt{3}$-Bi. The TPA layer appears as being composed by extended $[\bar{1}10]$-elongated stripes, as shown by lines in the right bottom corner of the figure. The width of these stripes is not uniform, being narrower in some regions indicated by "n" and wider in others indicated by "w", with an average value of about 2 nm. A very similar modulation of the TPA layer was also found on the $\sqrt{3}$-Ag surface [4].

Higher magnification STM images in Fig. 2(d)–(f) reveal that there are however slight differences in the adsorption geometry of individual TPA molecules on $\beta\sqrt{3}$-Bi in respect to $\sqrt{3}$-Ag. The images look somewhat blurred since the molecular layer appears to be

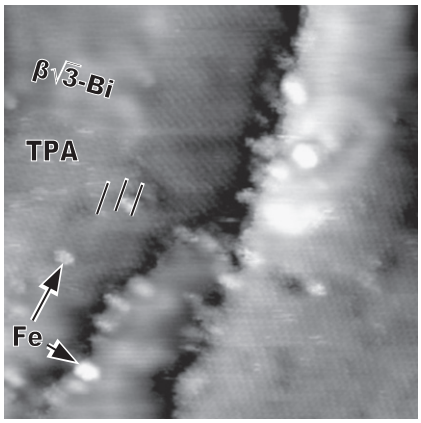

Fig. 3. STM image after Fe deposition onto the TPA layer. Fe-based clusters are explicitly indicated by arrows. Straight lines show the boundaries between unaltered "w" and "n" regions in the TPA domains. Sizes are 50×50 nm^2 ($V_s=-0.2$ V, I = 0.2 nA).

partially "transparent" in the whole examined range of negative sample voltages and the details and defects of the underlying $\beta\sqrt{3}$-Bi substrate get mixed with the molecular details (see arrowheads in Fig. 2(c)). Nevertheless, it is possible to identify individual molecules, which are characterized by three bright spots consistently observed inside each TPA, as indicated by three dots within a dashed ellipse in Fig. 2(d). This is consistent with a flat-lying absorption geometry which thus differs from what reported for pentacene on $\beta\sqrt{3}$-Bi [20]. Moreover, this observation allows us to determine the unit cells of the "n" and the "w" regions, indicated by a rectangle and a parallelogram, respectively, which turn out to be identical to those on the $\sqrt{3}$-Ag surface. On the $\beta\sqrt{3}$-Bi substrate, however, the $[\bar{1}\bar{1}2]$-oriented TPA molecular rows are located on top of the Bi trimer rows (see Fig. 2(d)), while they are in between the Si trimer rows on the $\sqrt{3}$-Ag surface [4].

A further difference is that on the $\beta\sqrt{3}$-Bi surface the individual TPA molecules can have different orientations with respect to the substrate, resulting in at least four different supramolecular structures. Three of them are indicated in Fig. 2(d)–(f) as TYPE Ia, Ib and Ic. In TYPE Ia domains, the TPA molecules are oriented along the $[\bar{1}\bar{1}2]$ substrate direction as can be seen in Fig. 2(d). However, in TYPE Ib domains, the molecules align close to $[\bar{1}01]$ while in TYPE Ic the molecular orientation is not fixed, as indicated by the ellipses in Fig. 2 (e) and (f), respectively. We note that the alternation of "n" and "w" regions as well as the symmetry of their unit cells is the same in all TYPE I regions, the orientation of the individual molecules being the only difference among the three. TPA molecules arrange also into a fourth type of domain, dubbed TYPE II, which however occurs with a lower frequency. Its structure is more complex than that of TYPE I, with molecules aligned both along $[\bar{1}\bar{1}2]$ and $[1\bar{2}1]$ and a random orientation (data not shown). The higher heterogeneity of the supramolecular structures formed by TPA on $\beta\sqrt{3}$-Bi in respect to $\sqrt{3}$-Ag and, in particular, the observed higher rotational freedom of the individual molecules hints at a lower surface–molecule interaction strength.

The STM measurements do not allow to precisely identify the type of intermolecular interaction responsible for the observed self-assembly. However, based on the functional moieties of TPA and on their planar arrangement, we speculate that the supramolecular layers are stabilized by hydrogen bonds. This is further supported by the similarity between the observed structures and those found on the $\sqrt{3}$-Ag surface [4].

The deposition of Fe onto the TPA layers results in the appearance of bright extended clusters which coexist with the unaltered TPA layers, as shown in Fig. 3. As for the $\sqrt{3}$-Ag surface, these clusters are most probably constituted of Fe or Fe-silicide and their formation does not allow the development of TPA-based 2D MOFs as otherwise reported on metallic surfaces. A substrate annealing up to 100 °C does not have any influence on the surface morphology leaving both the TPA layer and the Fe-based clusters unaltered.

By comparing the present studies with those performed on the Si 7×7 and the $\sqrt{3}$-Ag surfaces [4], we find that TPA molecules adsorb randomly on both the 7×7 and the $\alpha\sqrt{3}$-Bi surfaces while they form ordered supramolecular layers on both the $\sqrt{3}$-Ag and the $\beta\sqrt{3}$-Bi surfaces. These common behaviors are however not a reflection of a common surface structure. In fact, among the four substrates, only the 7×7 reconstruction has Si dangling bonds, while the $\sqrt{3}$-Ag includes both Ag and Si atoms in the topmost layer but no dangling bonds, and the $\alpha\sqrt{3}$-Bi and the $\beta\sqrt{3}$-Bi reconstructions do not even have Si surface atoms. In general, two main conditions must be satisfied for the formation of 2D supramolecular structures: a reversible non-covalent intermolecular interaction and a high surface mobility [7]. While the first evidently depends only on the TPA molecule, the second one does depend also on the chosen substrate. One of the main differences between the $\alpha\sqrt{3}$-Bi and the $\beta\sqrt{3}$-Bi reconstructions is the density of metal atoms in the topmost surface layer. The $\sqrt{3}$-Ag and the $\beta\sqrt{3}$-Bi surfaces have a 1ML coverage, while the $\alpha\sqrt{3}$-Bi surface has only 1/3ML coverage. As a consequence, the distance between the metal atoms in the topmost layer of the $\alpha\sqrt{3}$-Bi substrate (about 7 Å) is larger than on the other two substrates (about 4 Å). This has most probably a significant influence on the corrugation of the adsorption potential and therefore on the surface diffusivity of the TPA molecules. In particular, the molecular mobility is expected to be higher on the metallic denser $\beta\sqrt{3}$-Bi surface, therefore promoting the formation of supramolecular structures on this reconstruction.

4. Summary

TPA adsorption on the $\alpha\sqrt{3}$-Bi and the $\beta\sqrt{3}$-Bi surfaces was investigated by STM. The TPA molecules do not form an ordered supramolecular layer, but adsorb randomly on the $\alpha\sqrt{3}$-Bi surface as well as on the 7×7 surface. In contrast, the TPA molecules form an ordered supramolecular layer on the $\beta\sqrt{3}$-Bi surface similarly to the $\sqrt{3}$-Ag surface. We conclude that not only the absence of Si dangling bonds but also a sufficiently high metal coverage is a prerequisite for the formation of supramolecular layers on Si substrates.

Acknowledgments

We thank S.L. Tait, A. Langner, C. Ast and I. Gierz, for fruitful discussions, and W. Stiepany, P. Andler, M. Siemers and R. Chaikevitch for technical assistance. STM data were analyzed using the WSxM free software [25].

References

[1] S. Clair, S. Pons, A.P. Seitsonen, H. Brune, K. Kern, J.V. Barth, J. Phys. Chem. B 108 (2004) 14585.
[2] M.E. Cañas-Ventura, F. Klappenberger, S. Clair, S. Pons, K. Kern, H. Brune, T. Strunskus, Ch. Wöll, R. Fasel, J.V. Barth, J. Chem. Phys. 125 (2006) 184710.
[3] S. Stepanow, T. Strunskus, M. Lingenfelder, A. Dmitriev, H. Spillmann, N. Lin, J.V. Barth, Ch. Wöll, K. Kern, J. Phys. Chem. B 108 (2004) 19392.
[4] T. Suzuki, T. Lutz, D. Payer, N. Lin, S.L. Tait, G. Costantini, K. Kern, Phys. Chem. Chem. Phys. 11 (2009) 6498.
[5] M.A. Lingenfelder, H. Spillmann, A. Dmitriev, S. Stepanow, N. Lin, J.V. Barth, K. Kern, Chem. Eur. J. 10 (2004) 1913.
[6] S. Stepanow, M. Lingenfelder, A. Dmitriev, H. Spillmann, E. Delvigne, N. Lin, X. Deng, C. Cai, J.V. Barth, K. Kern, Nat. Mater. 3 (2004) 229.
[7] J.V. Barth, G. Costantini, K. Kern, Nature 437 (2005) 671.
[8] S. Clair, S. Pons, H. Brune, K. Kern, J.V. Barth, Angew. Chem. Int. Ed. 44 (2005) 7294.
[9] S. Clair, S. Pons, S. Fabris, S. Baroni, H. Brune, K. Kern, J.V. Barth, J. Phys. Chem. B 110 (2006) 5627.
[10] T. Classen, M. Lingenfelder, Y. Wang, R. Chopra, C. Virojanadara, U. Starke, G. Costantini, G. Fratesi, S. Fabris, S. de Gironcoli, S. Baroni, S. Haq, R. Raval, K. Kern, J. Phys. Chem. A 111 (2007) 12589.
[11] A. Langner, S.L. Tait, N. Lin, C. Rajadurai, M. Ruben, K. Kern, Proc. Natl. Acad. Sci. U. S. A. 104 (2007) 17927.
[12] S.L. Tait, Y. Wang, G. Costantini, N. Lin, A. Baraldi, F. Esch, L. Petaccia, S. Lizzit, K. Kern, J. Am. Chem. Soc. 130 (2008) 2108.

[13] Y. Wang, S. Fabris, G. Costantini, K. Kern, J. Phys. Chem. C 114 (2010) 13020.
[14] K.J. Wan, T. Guo, W.K. Ford, J.C. Hermanson, Phys. Rev. B 44 (1991) 3471.
[15] C. Park, R.Z. Bakhtizin, T. Hashizume, T. Sakurai, Jpn. J. Appl. Phys. 32 (1993) L290.
[16] R. Shioda, A. Kawazu, A.A. Baski, C.F. Quate, J. Nogami, Phys. Rev. B 48 (1993) 4895.
[17] S. Nakatani, T. Takahashi, Y. Kuwahara, M. Aono, Phys. Rev. B 52 (1995) R8711.
[18] R.H. Miwa, T.M. Schmidt, G.P. Srivastava, J. Phys. Condens. Matter 15 (2003) 2441.
[19] T.M. Schmidt, R.H. Miwa, G.P. Srivastava, Braz. J. Phys. 34 (2004) 629.
[20] J. Teng, J. Guo, K. Wu, E. Wang, J. Chem. Phys. 129 (2008) 034703.
[21] A. Al-Mahboob, J.T. Sadowski, Y. Fujikawa, K. Nakajima, T. Sakurai, Phys. Rev. B 77 (2008) 035426.
[22] T. Nagao, T. Doi, T. Sekiguchi, S. Hasegawa, Jpn. J. Appl. Phys. 39 (2000) 4567.
[23] S. Yaginuma, T. Nagao, J.T. Sadowski, M. Saito, K. Nagaoka, Y. Fujikawa, T. Sakurai, T. Nakayama, Surf. Sci. 601 (2007) 3593.
[24] Y. Makoudi, F. Palmino, E. Duverger, M. Arab, F. Chérioux, C. Ramseyer, B. Therrien, M.J.-L. Tschan, G. Süss-Fink, Phys. Rev. Lett. 100 (2008) 076405.
[25] I. Horcas, R. Fernández, J.M. Gómez-Rodríguez, J. Colchero, J. Gómez-Herrero, A.M. Baro, Rev. Sci. Instrum. 78 (2007) 013705.